

# Martensitic transition and magnetoresistance in a Cu-Al-Mn shape memory alloy. Influence of ageing.

Jordi Marcos, Antoni Planes and Lluís Mañosa  
*Departament d'Estructura i Constituents de la Matèria,  
 Facultat de Física,  
 Universitat de Barcelona.  
 Diagonal, 647, E-08028 Barcelona, Catalonia*

Amílcar Labarta and Bart Jan Hattink  
*Departament de Física Fonamental,  
 Facultat de Física,  
 Universitat de Barcelona.  
 Diagonal, 647, E-08028 Barcelona, Catalonia*

(Dated: February 1, 2008)

We have studied the effect of ageing within the miscibility gap on the electric, magnetic and thermodynamic properties of a non-stoichiometric Heusler Cu-Al-Mn shape-memory alloy, which undergoes a martensitic transition from a *bcc*-based ( $\beta$ -phase) towards a close-packed structure ( $M$ -phase). Negative magnetoresistance which shows an almost linear dependence on the square of magnetization with different slopes in the  $M$ - and  $\beta$ -phases, was observed. This magnetoresistive effect has been associated with the existence of Mn-rich clusters with the  $Cu_2AlMn$ -structure. The effect of an applied magnetic field on the martensitic transition has also been studied. The entropy change between the  $\beta$ - and  $M$ -phases shows negligible dependence on the magnetic field but it decreases significantly with annealing time within the miscibility gap. Such a decrease is due to the increasing amount of  $Cu_2MnAl$ -rich domains that do not transform martensitically.

PACS numbers: PACS numbers: 81.30.Kf, 75.80.+q, 64.75.+g

## I. INTRODUCTION

The shape-memory effect [1] is characteristic of certain alloys (the so-called shape-memory alloys), which exhibit a martensitic transition (MT) from an ordered *bcc*-phase ( $\beta$ -phase) towards a close-packed low-temperature phase ( $M$ -phase). This effect is related to unique thermomechanical properties such as the ability to recover from large permanent deformations produced in the  $M$ -phase by the reverse transition when temperature is increased. During the nineties a great deal of interest has been devoted to the study and development of magnetic shape-memory materials. This interest is mostly due to the possibility of a magnetic control of the shape-memory effect, which has been made evident in the ferromagnetic Ni-Mn-Ga alloy close to the Heusler composition  $Ni_2MnGa$  [2]. Furthermore, these materials have been shown to exhibit unexpected pretransitional behaviour [3].

The present paper deals with the study of the Cu-Al-Mn alloy. This Hume-Rothery material [4] shares a number of features with the Ni-Mn-Ga alloy system. It displays the same high-temperature crystallographic structure, a martensitic transformation with associated shape-memory effect and interesting magnetic properties. For Cu-Al-Mn, however, the martensitic transition occurs in a composition region far from the Heusler stoichiometry. For this composition range, the  $\beta$ -phase is only stable at high temperatures, but can be retained at low-temperature by means of suitable cooling. During this cooling the system develops an ordered  $L2_1$  structure

( $Fm\bar{3}m$ , Heusler symmetry) in two successive disorder-order transitions:  $A2$  ( $Im\bar{3}m$ )  $\rightarrow$   $B2$  ( $Pm\bar{3}m$ ) at  $T_{c1}$  and  $B2 \rightarrow L2_1$  at  $T_{c2}$  [5]. Upon further cooling it undergoes a martensitic transition at a temperature which is strongly composition dependent. This transition has a diffusionless nature which ensures that the atomic distribution of the  $L2_1$  phase is inherited by the  $M$ -phase. It is worth noting that this feature is common to all Cu-based shape-memory materials [6].

Magnetic properties arise from localized magnetic moments at Mn-atoms as occurs in the Ni-Mn-Ga system [7]. These magnetic moments are coupled through an oscillating effective interaction (RKKY interaction). AL-CHEMI (Atom Location by Channelling Enhanced Microanalysis) experiments [8] have shown that Mn atoms are located preferentially in one of the four distinguishable *fcc* sublattices of the  $L2_1$  structure (the 4b sites in Wyckoff notation). For this configuration, ferromagnetic coupling is dominant and close to the  $Cu_2AlMn$  composition the system is ferromagnetic. However, for non-stoichiometric alloys the 4b sites are not fully occupied by Mn-atoms and this results in magnetic disorder, which gives rise to different magnetic behaviour depending on the temperature range [9, 10]. Magnetic clustering has been suggested to be at the origin of the magnetoresistive properties recently reported in Cu-Al-Mn melt-spun ribbons [11, 12]. An interesting feature is the fact that a phase separation between  $Cu_3Al$ -rich and  $Cu_2AlMn$ -rich phases may occur below the  $L2_1$  ordering line. It is therefore expected that the magnetic and structural

properties of the system are sensitive to the temperature history of the material (i.e., ageing). In particular, isothermal annealing at a temperature within the miscibility gap will result in the growth of magnetic clusters. The existence of a miscibility gap was first reported for the  $\text{Cu}_3\text{Al} \rightarrow \text{Cu}_2\text{AlMn}$  pseudobinary composition line [13] and later confirmed for Cu-rich systems with a composition that slightly deviates from this line [14]. Interestingly, this composition range includes that for which Cu-Al-Mn displays a martensitic transition. Recently, it has been theoretically shown [15] that the influence of magnetic degrees of freedom on configurational phase stability is at the origin of this phase separation.

The present paper is aimed at experimentally studying the influence of magnetism on the martensitic transformation in Cu-Al-Mn. Since the magnetic properties of this material are expected to be sensitive to ageing, this effect will be studied. In particular, we focus on the study of magnetotransport and magnetic properties through the martensitic transition of bulk samples. The results will contribute to gain a deeper understanding of the magnetoelastic interplay, which will be studied at different levels of coupling.

The paper is organized as follows. In section II, the experimental details are outlined. Section III deals with the experimental results, which are discussed in section IV.

## II. EXPERIMENTAL DETAILS

Measurements were performed on a Cu-Al-Mn polycrystal (grain size  $\sim 100\mu\text{m}$ ) prepared by melting pure elements (99.99% purity). The nominal composition of the studied alloy is Cu; 22.8 at% Al; 9.0 at % Mn. From the ingot, rectangular specimens (approximately  $12 \times 4 \text{ mm}^2$  and 0.01 mm thick for resistance measurements or 0.5 mm for calorimetric and magnetic measurements) were first cut with a low-speed diamond saw and mechanically polished down to the desired thickness. All samples were annealed for 10 min at 1080 K and quenched in a mixture of ice and water. This fast cooling avoids precipitation of equilibrium phases, but enables the two ordering transitions to the  $B_2$  and  $L2_1$  structures to take place ( $T_{B_2} = 849$  K and  $T_{L2_1} = 795$  K [5]). The nominal martensitic transition temperature of as-quenched samples is  $T_M = 157 \pm 1$  K. For the studied composition the structure of the  $M$ -phase is  $18R$  [16]. This structure is monoclinic but it is usually described by a larger (approximately orthorhombic) unit cell containing 18 close-packed atomic planes along the c-axis [17].

Phase separation between  $\text{Cu}_3\text{Al}$ -rich and  $\text{Cu}_2\text{AlMn}$ -rich domains occurs under very slow cooling from high temperature. In the as-quenched specimens phase separation can be induced by means of post annealing within the miscibility gap. This process takes place at slow rates so that it is completely negligible at room temperature (even on a month time scale). In all cases, ageing consist

in annealing at a temperature  $T_a = 473$  K for selected times. We chose this temperature because it is located slightly below the limit of the miscibility gap for the studied composition. Actually, above 525 K no phase separation was detected, while 50 K below, the magnitude of the observed effects is similar, but they occur on a longer time scale.

Four kind of measurements were performed: electrical resistance under applied magnetic field, magnetization, ac-susceptibility and calorimetry. Electrical resistance was measured from 5 K up to 300 K using an ac four-probe method. For magnetization measurements a SQUID magnetometer was used. For calorimetric measurements a highly sensitive and fast response (around 20 s time constant) calorimeter, which was specifically designed for the study of solid-solid phase transitions, was utilized [18]. Calorimetric, magnetization and ac-susceptibility runs were performed through the martensitic transition in the range from 100 K to room temperature. Calorimetric measurements were carried out at a rate of 0.5 K/min, and pairs of data (calorimetric output and temperature) were recorded every 2 seconds. Ac-susceptibility measurements were performed at a frequency  $f = 66$  Hz.

## III. RESULTS

Electrical resistance measurements were carried out by first cooling the sample down to 5 K and then increasing the temperature in steps up to 300 K. At each plateau, the resistance  $R$  was measured at different values of the magnetic field  $\mathcal{H}$  at intervals of 345 Oe from 0 to 10 kOe, and at 2100 Oe intervals within the range from 10 to 50 kOe. The magnetoresistance  $MR$ , defined as the relative change of  $R$  with  $\mathcal{H}$ , is computed as:  $MR = [R(T, \mathcal{H}) - R(T, \mathcal{H} = 0)] / R(T, \mathcal{H} = 0)$ . In Fig.1,  $MR$  is plotted as a function of  $\mathcal{H}$  at selected temperatures for samples subjected to increasing annealing times at  $T_a$ . In all cases, the alloy exhibits negative magnetoresistance, i.e., the resistance decreases as magnetic field increases and the magnitude of the change is higher at low temperature. Actually, the maximum  $MR$ , of about 7%, was obtained at  $T \simeq 10$  K and  $\mathcal{H} = 50$  kOe for the as-quenched specimen. Overall, the effect of ageing is to reduce the  $MR$  at high fields. However, at low fields a small increase is observed, which is associated with the material becoming magnetically softer. For instance, the  $MR$  at  $T = 300$  K and  $\mathcal{H} = 10$  kOe increases from a practically null value for the as-quenched state to  $\sim 0.5\%$  for the long-term annealed state.

An interesting feature concerns the influence of the martensitic transition on the  $MR$ . This effect is better revealed by plotting the change of  $R$  with  $T$  across the MT at selected values of  $\mathcal{H}$ . This is shown in Fig. 2 for an as-quenched sample and for a sample aged for 300 min. The curves obtained are equivalent to those obtained directly by measuring  $R$  versus  $T$  under con-

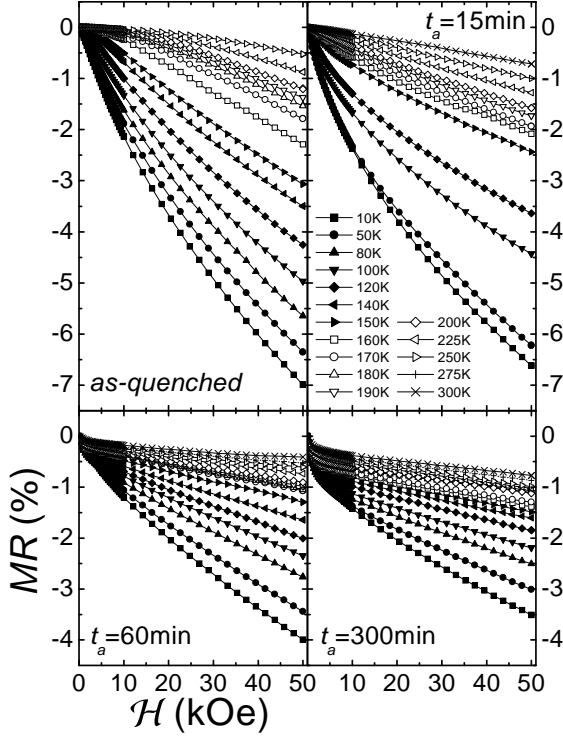


FIG. 1: Magnetoresistance  $MR$  versus magnetic field  $\mathcal{H}$  at selected temperatures and for different annealing times at  $T_a = 473$  K.

tinuous heating at different constant values of  $\mathcal{H}$  [20]. The large change in resistance in the temperature range between 150 K and 175 K for the as-quenched sample and between 175 K and 200 K for the annealed sample is due to the occurrence of the MT. We will take the temperature difference  $\Delta T$  between the maximum and the minimum of the  $R$  versus  $T$  curves as an estimation of the spread in temperature of the transition (difference in the starting and finishing transition temperatures). The corresponding change in resistance will be denoted by  $\Delta R$ . Regardless of the ageing influence, the effect of the magnetic field is mainly to decrease the resistance of the  $M$ -phase (the resistance in the  $\beta$ -phase decreases by a lower amount), which leads to a reduction in  $\Delta R$  as the field is increased. In addition,  $\Delta T$  is reduced when the field increases (in the as-quenched system this reduction amounts to  $\sim 6$  K for an applied field of 50 kOe).

In order to characterize the magnetic response of the system we carried out magnetization ( $\mathcal{M}$ ) and ac-susceptibility ( $\chi$ ) measurements through the martensitic transition. These measurements were undertaken on samples subjected to increasing annealing times at  $T_a$ . Figure 3(a) shows  $\mathcal{M}$  versus  $T$  curves at selected values of the magnetic field. Figure 3(b) shows magnetization versus  $\mathcal{H}/T$  curves. It is interesting to correlate the magnetization with the behaviour of the magnetoresistance. Figure 4 shows the  $MR$  as a function of the square of

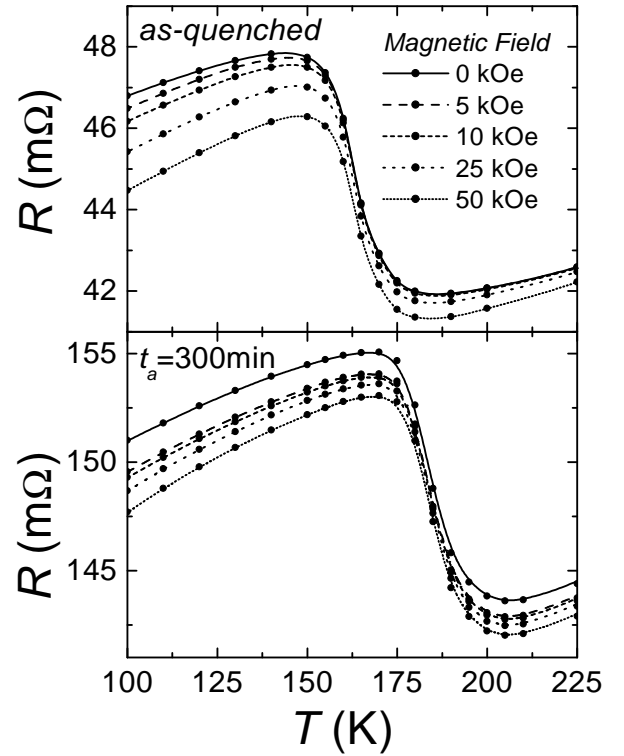
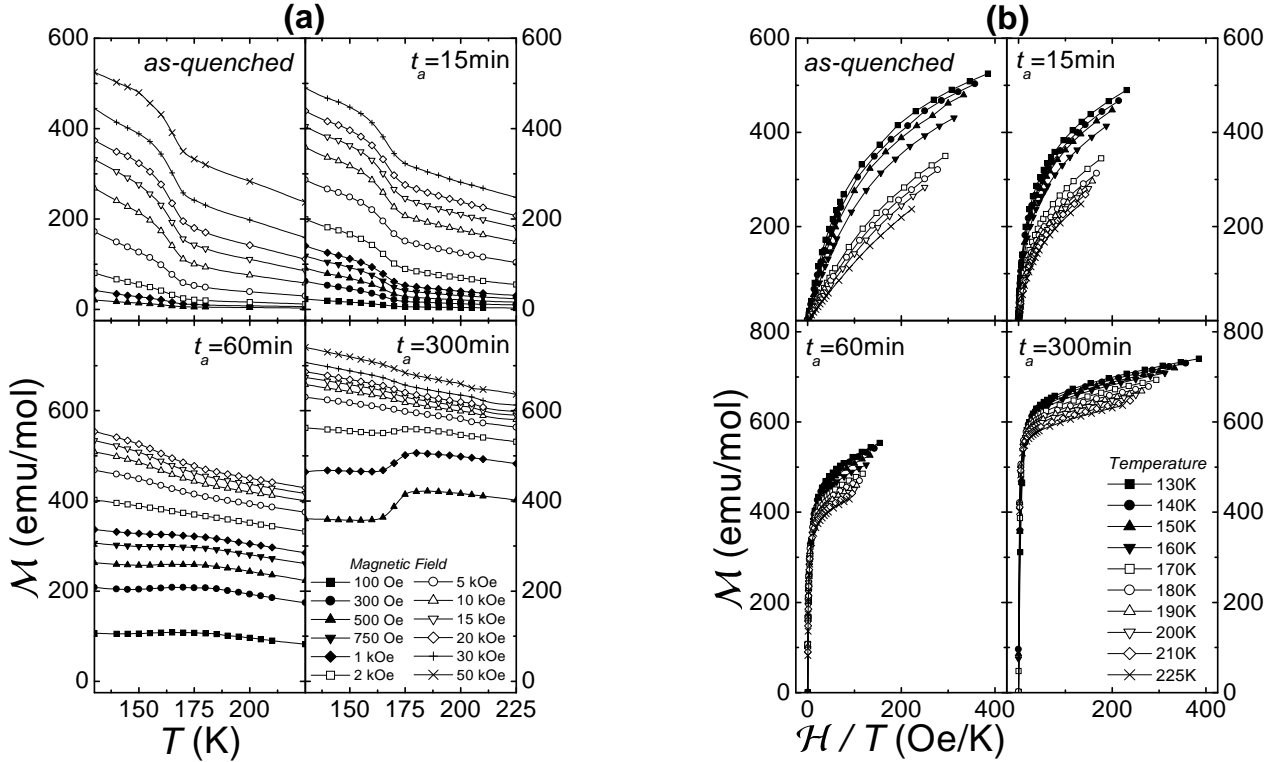


FIG. 2: Electrical resistance  $R$  versus temperature  $T$  at selected values of the magnetic field  $\mathcal{H}$  for an as-quenched sample and for a sample annealed 300 min at  $T_a = 473$  K.

magnetization  $\mathcal{M}^2$  for as-quenched and long-term aged specimens. For each sample, all data for the  $\beta$ -phase scale on a single curve, while data for the  $M$ -phase scale on another curve. In the as-quenched state, the two scaling curves are approximately linear, while remarkable deviations from linearity are evident in the annealed system, particularly for high values of  $\mathcal{M}$ . Moreover, in the annealed state, the scaling (in both  $\beta$ - and  $M$ -phases) is not as good as in the as-quenched state.

As illustrated in Fig. 3(a), magnetization curves show a significant change  $\Delta \mathcal{M}$  at the MT ( $\Delta \mathcal{M}$  is estimated as the magnetization difference at the transition temperature between extrapolations of the linear behaviour of  $\mathcal{M}$  versus  $T$  curves well above and well below the transition). Fig. 5 gives  $\Delta \mathcal{M}$  versus  $\mathcal{H}$  after different annealing times at  $T_a$ . In the as-quenched state,  $\Delta \mathcal{M}$  saturates for a value of  $\mathcal{H}$  close to 20 kOe; the field needed to reach saturation decreases with increasing annealing time. In all cases, for these values of the field, the magnetization itself is far from having reached saturation. Moreover, the saturation value of  $\Delta \mathcal{M}$  ( $\Delta \mathcal{M}_{sat}$ ) is strongly dependent on the annealing time. Actually, it decreases with  $t_a$  as shown in the inset of Fig. 5, reaching, within error, a constant value for  $t_a > 150$  min.

As the MT is first order, any change of the temperature  $T_M$  induced by the applied magnetic field  $\mathcal{H}$  should



be accounted for by the Clausius-Clapeyron equation

$$\frac{dT_M}{dH} = -\frac{\Delta\mathcal{M}}{\Delta S}, \quad (1)$$

where  $\Delta S$  is the entropy difference between  $M$ - and  $\beta$ -phases. We measured  $\Delta S$  using calorimetry after different annealing times. In Fig. 6, we present thermal curves obtained during heating runs for different annealing times. These curves show the characteristic noisy structure which is common to many martensitic transitions [21, 22]. Such a noisy structure is enhanced in the as-quenched state. As the annealing time increases, the transformation first becomes smoother and broader, and shifts towards lower temperatures. However, for times longer than 90 min thermal curves partially recover the original noisy character and the transformation shifts towards higher temperatures. The entropy change is determined by a numeric integration of the thermograms [23]. The value obtained for the as-quenched system ( $1.27 \pm 0.02$  J/Kmol) is consistent with that reported in [24]. The dependence of  $\Delta S$  on  $t_a$  is depicted in Fig. 7. The figure reveals that  $\Delta S$  (absolute value) decreases when the annealing time at  $T_a$  increases, reaching (as occurs with  $\Delta\mathcal{M}_{sat}$ ) a constant value for  $t_a > 150$  min. The relative decrease of  $\Delta S$  is about 30%, much smaller than the relative decrease  $\Delta\mathcal{M}_{sat}$ , which is estimated to be approximately 90%.

It is then interesting to compare the values of the derivative  $dT_M/dH$  in the as-quenched and long-term annealed states using equation 1. For the as-quenched system, a value of  $(8 \pm 0.4)$  mK/kOe is obtained, while

FIG. 3: (a) Magnetization  $\mathcal{M}$  versus temperature  $T$  at selected values of  $H$  for different annealing times at  $T_a = 473$  K. (b) Magnetization as a function of  $H/T$  for several selected temperatures; solid symbols correspond to the  $M$ -phase and open symbols to the  $\beta$ -phase.

this value reduces to  $(1.10 \pm 0.05)$  mK/kOe after 300 min of annealing. The reduction is mainly related to the decrease of  $\Delta\mathcal{M}_{sat}$  with ageing. Actually, the derivative  $dT_M/dH$  provides a good quantification of the dependence of the structural transition temperature on a magnetic field under the assumption that  $\Delta S$  is independent of  $H$ . Such an assumption is based on the fact that the entropy difference between the open and close-packed phases originates from the change of the corresponding vibrational spectrum, as occurs in non-magnetic Cu-based shape-memory alloys [25].

A possible magnetic contribution to  $\Delta S$  can be evaluated from the magnetization vs. temperature curves. Actually, at a given temperature  $T$ , the change of entropy of the system with the magnetic field  $H$  is given by:

$$\delta S(T, H) \equiv S(T, H) - S(T, H=0) = \int_0^H \left( \frac{\partial \mathcal{M}}{\partial T} \right)_H dH, \quad (2)$$

where the thermodynamic (Maxwell) relation:

$$\left( \frac{\partial S}{\partial H} \right)_T = \left( \frac{\partial \mathcal{M}}{\partial T} \right)_H, \quad (3)$$

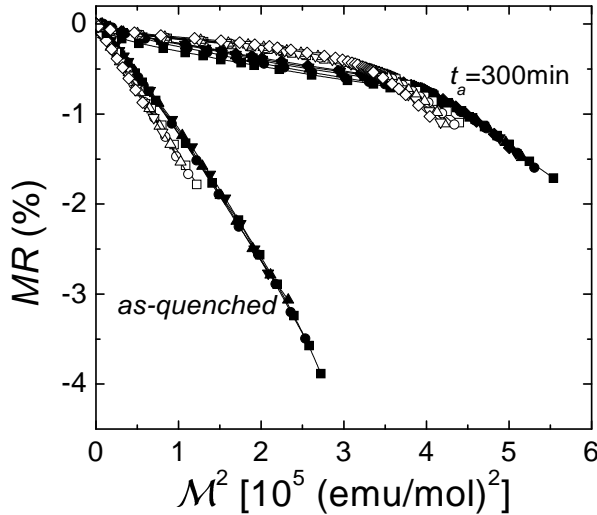


FIG. 4: Magnetoresistance  $MR$  as a function of the square of the magnetization. Solid symbols correspond to the  $M$ -phase and open symbols, to the  $\beta$ -phase. Results for an as-quenched and a long-term aged ( $t_a = 300$  min) specimen are shown.

has been used. Therefore, application of a magnetic field modifies the entropy change between both the  $M$ - and  $\beta$ -phases according to:

$$\begin{aligned} \delta\Delta S &= \Delta S(\mathcal{H}) - \Delta S(\mathcal{H} = 0) \\ &= \int_0^{\mathcal{H}} \left[ \left( \frac{\partial \mathcal{M}^M}{\partial T} \right)_H - \left( \frac{\partial \mathcal{M}^\beta}{\partial T} \right)_H \right] d\mathcal{H}, \end{aligned} \quad (4)$$

where  $\left( \frac{\partial \mathcal{M}^M}{\partial T} \right)_H$  and  $\left( \frac{\partial \mathcal{M}^\beta}{\partial T} \right)_H$  are the derivatives of the magnetization with respect to the temperature in the  $M$ - and  $\beta$ -phases. The preceding integral was calculated numerically from the magnetization curves above following the procedure given in [26]. Results are plotted in Fig. 8 as a function of  $\mathcal{H}$  for different annealing times. This quantity is always negative, which means that the effect of the field is to increase the absolute value of  $\Delta S$ . However, the increase is very small, and represents, in all cases, less than 1% of the total entropy change. It can therefore be considered negligible for practical purposes. It is, however, interesting to compare this entropy difference with that reported in a Ni<sub>51.5</sub>Mn<sub>22.7</sub>Ga<sub>25.8</sub> polycrystalline alloy [27]. In that case a value of  $\delta\Delta S \sim -4 \times 10^{-3}$  J/K mol is estimated at  $\mathcal{H} = 0.9$  T. This value is comparable with the value reported here for the Cu-Al-Mn system. Notice that for the Ni-Mn-Ga system, the change in MT temperature with magnetic field is also very weak [25].

An additional, complementary magnetic characterization of the studied system consisted of measuring the ac magnetic susceptibility as a function of the ageing time  $t_a$ . The evolution of the real part of the ac-susceptibility is displayed in Fig. 9. In the as-quenched state, the magnetic susceptibility is small and shows a low-temperature

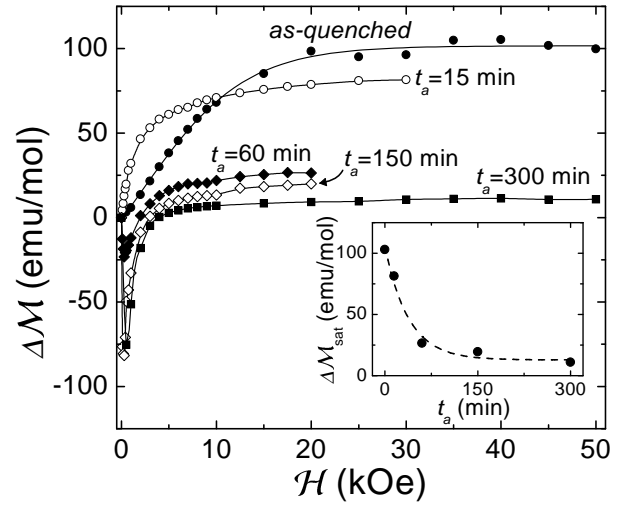


FIG. 5: Magnetization change  $\Delta\mathcal{M}$  at the martensitic transition versus magnetic field  $\mathcal{H}$  at selected annealing times at  $T_a = 473$  K. The inset shows the saturation value of  $\Delta\mathcal{M}$  as a function of annealing time (the dashed line is a guide to the eye).

peak associated with the appearance of a glassy magnetic phase. The martensitic transition can be detected on this curve as a very small jump between 160 K and 170 K. The inset of the figure shows a detailed view of the region where the MT takes place. In this case, heating and cooling runs are presented so that the transformation hysteresis is revealed.

As ageing time is increased, the susceptibility peak moves towards higher temperatures and becomes simultaneously higher and broader. Besides, the evolution of the martensitic transition temperature with  $t_a$  follows that of the evolution determined from the calorimetric measurements presented above. For annealing times  $t_a > 60$  min the anomalies associated with the freezing temperature and the martensitic (jump) phases overlap. This fact gives rise to a susceptibility that decreases abruptly at an intermediate temperature ( $\sim 150$  K) as temperature is reduced. With further annealing, the shape of the susceptibility curves remains unchanged, but the value of  $\chi$  decreases at high temperatures indicating that the system becomes more and more ferromagnetic.

#### IV. DISCUSSION

In this paper, we have reported results showing the existence of magnetoresistive effects in bulk polycrystalline Cu-Al-Mn samples. Magnetoresistive behaviour had already been observed in  $\beta$ -phase melt-spun ribbons of similar composition [14]. In the present paper, the investigation has been extended to the bulk system and to the study of magnetoresistance in the martensitic phase. In both  $\beta$ - and  $M$ -phases, the observed magnetoresistance

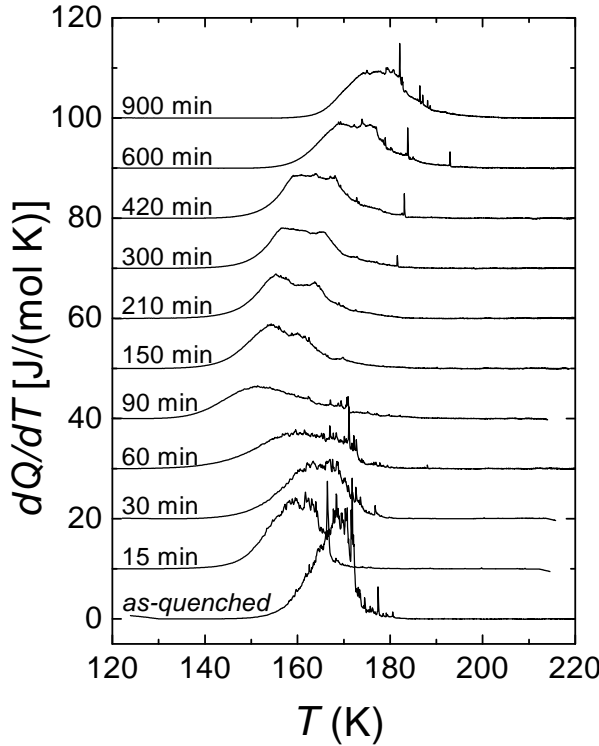


FIG. 6: Thermal curves corresponding to the reverse (heating) martensitic transition obtained after different annealing times at  $T_a = 473$  K.

is typical of heterogeneous alloys [28] where magnetoresistance originates from the spin-dependent scattering of conduction electrons on ferromagnetic clusters embedded in a metallic non-magnetic matrix [29]. In the studied system, the ferromagnetic clusters are due to the tendency of Mn-atoms to increase their number of third-order neighbours of the same species within the basic *bcc*-lattice. At present there is substantial experimental evidence of the existence of these clusters [13, 14]. X-ray experiments [5] have demonstrated that quenched samples exhibit an  $L_2$  structure. In this structure, the Mn-atoms are preferentially located on the 4b sites (Wyckoff notation) of the cubic unit cell of the  $Fm\bar{3}m$  structure. However, the distribution of Mn atoms in this sublattice is not completely random. Actually, there are indications of the existence of correlations among the positions of the Mn-atoms within the sublattice [9]. While clusters are not strictly well defined in this case, their influence on transport and magnetic properties of the system has to be considered. In particular, they are responsible for the superparamagnetic behaviour of the studied alloy system, as shown in [10]. The clustering tendency is enhanced by ageing within the miscibility gap. Actually, the influence of ageing on the magnetic properties of Cu-Al-Mn shows up by the remarkable effect that ageing has on the *MR* curves; a decrease in the magnitude of *MR* at low temperatures and a slight increase at high temperatures

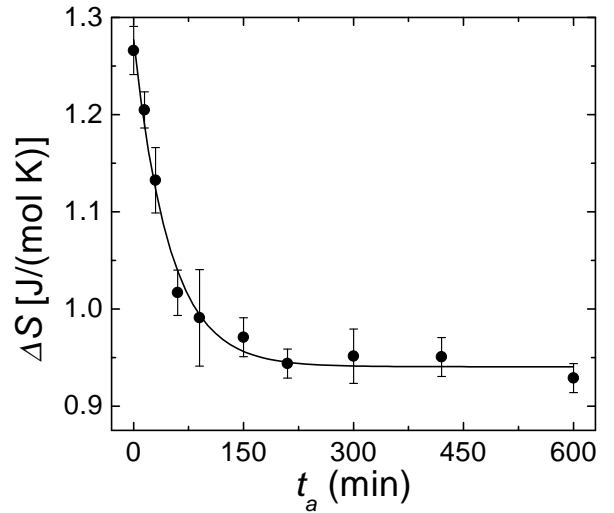


FIG. 7: Entropy change between *M*- and  $\beta$ -phases as a function of ageing time at  $T_a = 473$  K. The solid line corresponds to an exponential decay fitted function and serves as a visual guide.

have been observed (see Fig. 1). These modifications are due to an increase in the magnetic softening which takes place after short annealing times. This is clearly a sign of the increase of the ferromagnetic character of the system owing to the growth of magnetic clusters. Such an increase is confirmed by magnetization and susceptibility measurements.

The scaling of *MR* with  $\mathcal{M}^2$  was found to be different in both the  $\beta$ - and *M*-phases. This effect mainly arises from the different behaviour of the magnetization in the two phases. Actually, the  $\mathcal{M}$  vs.  $\mathcal{H}/T$  curves also show a tendency to group into two different families corresponding to the  $\beta$ - and *M*-phases, respectively. In the as-quenched state, the *MR* shows a fairly good linear dependence on  $\mathcal{M}^2$  for both the  $\beta$ - and *M*-phases. This is the expected behaviour in the absence of magnetic interaction between magnetic clusters [30]. However, at high fields the curves for the *M*-phase show a clear tendency to deviate from linear behaviour. A similar deviation has previously been observed in heterogeneous alloys and it has been attributed to the progressive field alignment of the disordered spins at the boundaries of the magnetic clusters, which causes a large variation of the *MR* compared with the corresponding change in magnetization [31]. Such an increase in the slope of the *MR* vs.  $\mathcal{M}^2$  curves is usually associated with the existence of high values of the high field susceptibility, as is the case of the as-quenched and short-term annealed samples [see magnetization curves in Fig. 3(b)]. After long time annealing, ferromagnetism is responsible for the loss of linearity in the *MR* versus  $\mathcal{M}^2$  curves. Actually, the formation of large ferromagnetic clusters whose magnetization saturates at relatively low fields (see Fig. 3(b)) leads to a

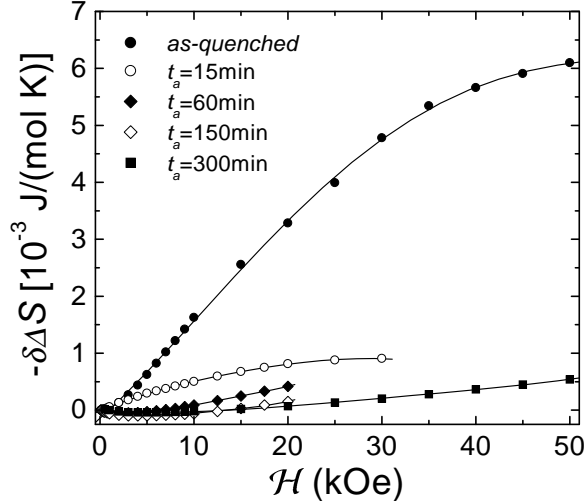


FIG. 8: Change in the entropy difference between  $\beta$  and  $M$  phases  $-\delta\Delta S$ , as a function of the magnetic field  $\mathcal{H}$  after different annealing times at  $T_a = 473$  K.

large change of the total magnetization of the sample and a small variation of  $MR$  at low fields, since the latter originates from the moment alignment of the small clusters and/or the spins at the boundaries of the ferromagnetic regions, which occurs at higher fields. Consequently,  $MR$  vs.  $M^2$  shows a quasi-constant regime that corresponds to the range of fields in which the magnetic saturation of large ferromagnetic clusters takes place (see Fig. 4) and a subsequent quasi-linear behaviour due to the magnetoresistance associated with small clusters and boundary spins.

A noticeable effect of the magnetic field on the martensitic transition is the reduction of the temperature range  $\Delta T$  in which the transition occurs. A qualitatively comparable effect has been reported in the case of the ferromagnetic  $\text{Ni}_2\text{MnGa}$  [2], but in this material the reduction is much greater; for that alloy the transition range reduces from about 10 K without an applied magnetic field to less than 2 K for an applied field of 10 kOe. In shape-memory alloys, the transformation is acknowledged to be thermoelastic, which means that the system needs to be continuously cooled down (or heated up) in order to increase the transformed fraction of the new phase. The transition is not completed until the temperature is lowered (increased) below (above) a certain value. The free-energy difference between both phases provides the driving force for the transition. Such a driving force is proportional to the temperature difference between equilibrium and the actual temperature to a first approximation [32]. The path followed by the system is an optimal path in which accommodation of the transformation elastic strain is almost accomplished. Therefore,  $\Delta T$  represents a reasonable measure of the stored elastic energy during the forward transformation [23]. From this point of view, a decrease in  $\Delta T$  reflects a lower value

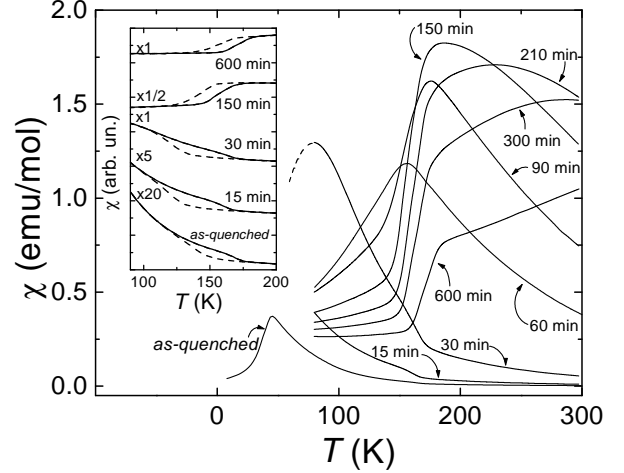


FIG. 9: Evolution of the real part of the ac magnetic susceptibility  $\chi$  with annealing times at  $T_a = 473$  K. The inset shows a detailed view of the temperature region where the martensitic transition takes place. Both heating (solid line) and cooling (dashed line) runs are displayed, revealing the transformation hysteresis. For clarity, the curves have been magnified by a factor that is indicated on each curve.

of this stored elastic energy. We argue that the physical mechanism behind this effect is that the magnetic field around magnetic clusters breaks the degeneracy of the low-temperature martensitic phase thus favouring the nucleation of these variants with the magnetization easy-axis in the direction of the field. In Cu-Al-Mn, approximately orthorhombic martensitic domains, with the  $c$ -axis oriented along the magnetic field, are expected to have maximum nucleation probability. In the Ni-Mn-Ga alloy such an interpretation is corroborated by the fact that magnetic and mechanical energies required to induce a single variant martensitic structure from a polyvariant crystal are comparable [33].

An interesting result concerns the magnetization jump occurring at the martensitic transition. This jump is positive (increase of the magnetization in the forward transition from the  $\beta$ - to the  $M$ -phase) in the as-quenched state even for small fields. However, for sufficiently long annealing time, when the sample behaves ferromagnetically, this jump is negative for small values of the field and becomes positive above a certain critical field close to the value for which  $\Delta M$  saturates. This is related to a high magnetic moment of the Mn-clusters and to the strong magnetic anisotropy of the martensitic phase. For fields larger than the critical field, reorientation of martensitic variants enables the Zeeman energy to be minimized and the jump again becomes positive.

The behaviour of magnetic susceptibility provides further understanding of the origin of the interplay between magnetic and structural degrees of freedom. In the as-quenched state, the temperature dependence of the ac-susceptibility is that which is expected for a system with

magnetic clusters. Below a freezing temperature (maximum of the  $\chi$  versus  $T$  curve) the large magnetic moments of  $L2_1$ -clusters are frozen along the magnetic easy axis. When the ageing time is increased, the peak associated with the occurrence of the frozen magnetic phase shifts towards higher temperatures and becomes broader. This is a consequence of the sensitivity of the susceptibility to the size and shape distribution of the magnetic clusters. For annealing times longer than  $\sim 100$  min the behaviour of the susceptibility is that expected for a ferromagnetic system: it is quite constant in both  $M$ - and  $\beta$ -phases. In the temperature range where the  $MT$  takes place, the increase in the ferromagnetic correlation among clusters explains the evolution of the shape of the hysteresis cycle of the  $MT$  with an increase of ageing time. For short ageing times,  $\chi$  increases at the  $MT$  (forward transition) due to the tendency of the magnetic moments to freeze. In contrast, when the system becomes ferromagnetic, the behaviour of  $\chi$  at the transition is dominated by the magnetic anisotropy which is larger in the  $M$ - than in the  $\beta$ -phase.

From a general viewpoint, the results discussed above must be considered as evidence of the coupling between magnetic and structural degrees of freedom occurring at a mesoscopic scale, that is at the length scale of the magnetic/martensitic domains. The coupling also exists at a microscopic level (spin-phonon coupling) which is made clear by the estimated (through Clausius-Clapeyron equation) change of  $T_M$  with  $\mathcal{H}$ . This coupling is however very weak and is related to the small magnetic contribution to the entropy difference between the  $\beta$ - and  $M$ -phases. The obtained value is comparable to that estimated for ferromagnetic Ni-Mn-Ga, but is considerably smaller than the value ( $\sim 0.1$  K/kOe) reported for ferrous martensitic alloys [34]. Consistently, it has been shown that application of a magnetic field does not significantly

modify the phonon branches in Ni-Mn-Ga [35].

At this point, it is worth noticing that the strong influence of ageing on the entropy difference between  $\beta$ - and  $M$ -phases may not be related to an increase in the magnetic contribution to the entropy. This effect must be simply ascribed to the fact that Mn-rich regions do not transform martensitically. The important change of  $\Delta S$  takes place within the ageing time interval during which the system becomes ferromagnetic. Notice that simultaneously the magnetization change at the transition reaches its saturation value. Therefore, any further evolution of the magnetic properties (as, for instance, revealed by ac-susceptibility measurements) of the system are originated by short-range reordering processes.

To conclude, the results presented prove the existence of both magnetoresistive and magnetoelastic properties in a non-stoichiometric Heusler Cu-Al-Mn alloy with a Mn content of 9 at% and with shape-memory properties. The occurrence of a martensitic transition has enabled the study of the effect of the crystallographic structural change on the above mentioned properties. The magnetoresistive behaviour has been shown to be different for the two structures. With regards to magnetoelastic coupling, it has been found that it mainly occurs at a mesoscopic level between martensitic domains and magnetic clusters.

## Acknowledgments

This work has received financial support from the CI-CyT (Spain), projects MAT2001-3251, MAT2000-0858 and from CIRIT (Catalonia), project 2001SGR00066. J.M. is supported by Direcció General de Recerca (Generalitat de Catalunya).

---

- [1] *Shape Memory Materials*, edited by K. Otsuka and C.M. Wayman, Cambridge University Press, Cambridge 1998.
- [2] K. Ullakko, J.K. Huang, C. Kantner, V.V. Kokorin and R.C. O'Handley, *Appl. Phys. Lett.*, **69**, 13 (1996); S.J. Murray, M. Marioni, S.M. Allen, and R.C. O'Handley, *Appl. Phys. Lett.*, **77**, 886 (2000).
- [3] A. Zheludev, S.M. Shapiro, P. Wochner, A. Schwartz, M. Wall and L.E. Tanner, *Phys. Rev. B*, **51**, 11310 (1995); A. Planes, E. Obradó, A. González-Comas, Ll. Mañosa, *Phys. Rev. Lett.*, **79**, 3926 (1997).
- [4] The phase stability of Hume-Rothery materials is largely dominated by the average number of conduction electrons per atom; see for instance M. Ahlers, *Z. Phys. B* **99**, 491 (1996).
- [5] E. Obradó, C. Frontera, Ll. Mañosa, and A. Planes, *Phys. Rev. B* **58**, 14245 (1998).
- [6] M. Ahlers, *Prog. Mater. Sci.*, **30**, 135 1986.
- [7] P.J. Webster and K.A.R. Ziebeck, in *Heusler alloys, Landolt Bornstein New Series Vol III (19c)* ed. by O. Madelung (Springer-Verlag, Berlin 1988) p- 75.
- [8] N. Nakanishi, T. Shigematsu, N. Machida, K. Ueda, K. Shimizu, Y. Nakata, *Proc. Int. Conf. on Martens. Transf.*, Monterey 1993, Ed. by J. Perkins and C.M. Wayman, p. 581
- [9] M.O. Prado, F.C. Lovey, and L. Civale, *Acta Mater.* **46**, 137 (1998).
- [10] E. Obradó, A. Planes, and B. Martínez, *Phys. Rev. B* **59**, 11450 (1999).
- [11] A.S. Murthy, L. Yiping, G.C. Hadjipanayis, and K.R. Lawless, *IEEE Trans. Mag.* **31**, 3958 (1995).
- [12] S. Sugimoto, S. Kondo, H. Nakamura, D. Book, Y. Wang, T. Kagotani, R. Kainuma, K. Ishida, M. Okada, and M. Homma, *J. Alloys Comp.* **265**, 273 (1998).
- [13] M. Bouchard and G. Thomas, *Acta metall.*, **23**, 1485 (1975).
- [14] R. Kainuma, N. Satoh, X.J. Liu, I. Ohnuma, and K. Ishida, *J. Alloys Comp.* **266**, 191 (1998).
- [15] J. Marcos, E. Vives and T. Castán, *Phys. Rev. B*, **63**, 224418-1 (2001).
- [16] E. Obradó, Ll. Mañosa and A. Planes, *Phys. Rev. B*, **56**,

20 (1997).

[17] F. C. Lovey, *Acta Metall.*, **35**, 1103 (1987).

[18] A simplified version of the calorimeter is described in Ll. Mañosa, M. Bou, C. Calles, and A. Cirera, *Am. J. Phys.*, **64**, 283 (1996).

[19] J. Marcos, L. Castro, A. Planes, Ll. Mañosa, and R. Romero, unpublished results.

[20] J. Marcos, A. Planes, Ll. Mañosa, A. Labarta, B.J. Hattink, *J. Phys. IV (France)* **11**, Pr8-257 2001.

[21] P.C. Clapp, *J. Phys. IV (France)* **C8**, C8-11 1995.

[22] E.M. Levin, V.K. Pecharsky and K.A. Gschneidner, Jr., *Phys. Rev. B* **63**, 174110 (2001).

[23] J. Ortín and A. Planes, *Acta metall.*, **36**, 1873 (1988).

[24] M.O. Prado, P.M. Decorte and F. Lovey, *Scr. metall. mater.*, **33**, 877 (1995).

[25] A. Planes and Ll. Mañosa, *Solid State Physics*, **55**, 159 (2001).

[26] V.K. Pecharsky and K.A. Gschneidner, *J. Appl. Phys.*, **86**, 565 (1999).

[27] F. Hu, B. Shen and J. Sun, *Appl. Phys. Lett.*, **76**, 3460 (2000).

[28] A.E. Berkowitz, J.R. Mitchell, M.J. Carey, A.P. Young, S. Zhang, F.E. Spada, F.T. Parker, H. Hutten and G. Thomas, *Phys. Rev. Lett.*, **68**, 3745 (1992); J.Q. Xiao, J.S. Jiang and C. Chien, *Phys. Rev. Lett.*, **68**, 3749 (1992).

[29] R.E. Camley and J. Barnes, *Phys. Rev. Lett.*, **63**, 644 (1989); P.M. Levy, S. Zhang and A. Fert, *Phys. Rev. Lett.*, **65**, 1643 (1990).

[30] J.-Q. Wang and G. Xiao, *Phys. Rev. B*, **49**, 3982 (1994).

[31] G. Bellouard, B. Geoge, and G. Marchal, *J. Phys. Condens. Matter*, **6**, 7239 (1994).

[32] The equilibrium temperature is defined as the non-constrained co-existence temperature of the  $\beta$ - and  $M$ -phases. Since hysteresis is small in such a class of transition, this temperature is close to the temperature of the onset of the forward transition and end of the reverse transition.

[33] R.C. O'Handley, *J. Appl. Phys.*, **83**, 3263 (1998).

[34] T. Kakeshita, K. Shimizu, S. Funada and M. Date, *Acta metall.*, **33**, 1381 (1985).

[35] Ll. Mañosa, A. Planes, J. Zarestky, T. Lograsso, D.L. Schlagel, and C. Stassis, *Phys. Rev. B*, **64**, 024305 (2001).